

Research



Cite this article: McDevitt-Galles T, Moss WE, Calhoun DM, Johnson PTJ. 2020 Phenological synchrony shapes pathology in host–parasite systems. *Proc. R. Soc. B* **287**: 20192597. <http://dx.doi.org/10.1098/rspb.2019.2597>

Received: 6 November 2019

Accepted: 28 December 2019

Subject Category:

Ecology

Subject Areas:

ecology

Keywords:

phenology, mismatch–match, amphibian decline, disease ecology, climate change

Author for correspondence:

Travis McDevitt-Galles

e-mail: travis.mcdevittgalles@colorado.edu

Electronic supplementary material is available online at <https://doi.org/10.6084/m9.figshare.c.4805622>.

Phenological synchrony shapes pathology in host–parasite systems

Travis McDevitt-Galles¹, Wynne E. Moss¹, Dana M. Calhoun^{1,2} and Pieter T. J. Johnson¹

¹Ecology and Evolutionary Biology, University of Colorado, Boulder, CO, USA

²United States Geological Survey, National Wildlife Health Center, 6006 Schroeder Road, Madison, WI 53711, USA

TM-G, 0000-0002-4929-5431; WEM, 0000-0002-2813-1710; DMC, 0000-0002-9483-2064; PTJJ, 0000-0002-7997-5390

A key challenge surrounding ongoing climate shifts is to identify how they alter species interactions, including those between hosts and parasites. Because transmission often occurs during critical time windows, shifts in the phenology of either taxa can alter the likelihood of interaction or the resulting pathology. We quantified how phenological synchrony between vulnerable stages of an amphibian host (*Pseudacris regilla*) and infection by a pathogenic trematode (*Ribeiroia ondatrae*) determined infection prevalence, parasite load and host pathology. By tracking hosts and parasite infection throughout development between low- and high-elevation regions (San Francisco Bay Area and the Southern Cascades (Mt Lassen)), we found that when phenological synchrony was high (Bay Area), each established parasite incurred a 33% higher probability of causing severe limb malformations relative to areas with less synchrony (Mt Lassen). As a result, hosts in the Bay Area had up to a 50% higher risk of pathology even while controlling for the mean infection load. Our results indicate that host–parasite interactions and the resulting pathology were the joint product of infection load and phenological synchrony, highlighting the sensitivity of disease outcomes to forecasted shifts in climate.

1. Introduction

Ongoing shifts in climate are altering the timing of key life-history events for species across the globe [1–3]. Already, a broad range of biological phenomena exhibit shifts in their phenology [4], including first flowering date [5], insect emergence [6], amphibian breeding [7], and the departure or arrival date of migratory birds [8]. While the overarching trend is advancements, species vary considerably in both the magnitude and direction of responses as a function of geographical location, life history and the specific environmental cues used (e.g. temperature versus day length) [9]. Importantly, variable responses among species can also lead to changes in the strength of species interactions or even result in novel species interactions [10,11]. For example, warmer Arctic spring temperatures—which have advanced the fruiting of elderberries by several weeks—led to a shift in brown bear dietary preferences, ultimately reducing predation on salmon and diminishing the indirect effects of salmon carcasses for riparian ecosystems [12]. Anticipating the effects of climate shifts for ecological communities thus requires quantification of how phenological overlap mediates interactions across a broad spectrum of taxa, trophic levels and spatial scales.

Shifts in climate also have the potential to alter interactions between hosts and parasites, which have important implications for disease risk in humans [13], wildlife [14] and crops [15]. Yet due to the complex life cycles and alternative transmission pathways of numerous parasites, forecasting the indirect effects of climate change, including phenological shifts in host or parasite taxa, has remained a persistent challenge [16,17]. For many host and parasite taxa, both the likelihood of infection and its pathological outcomes are highly sensitive to

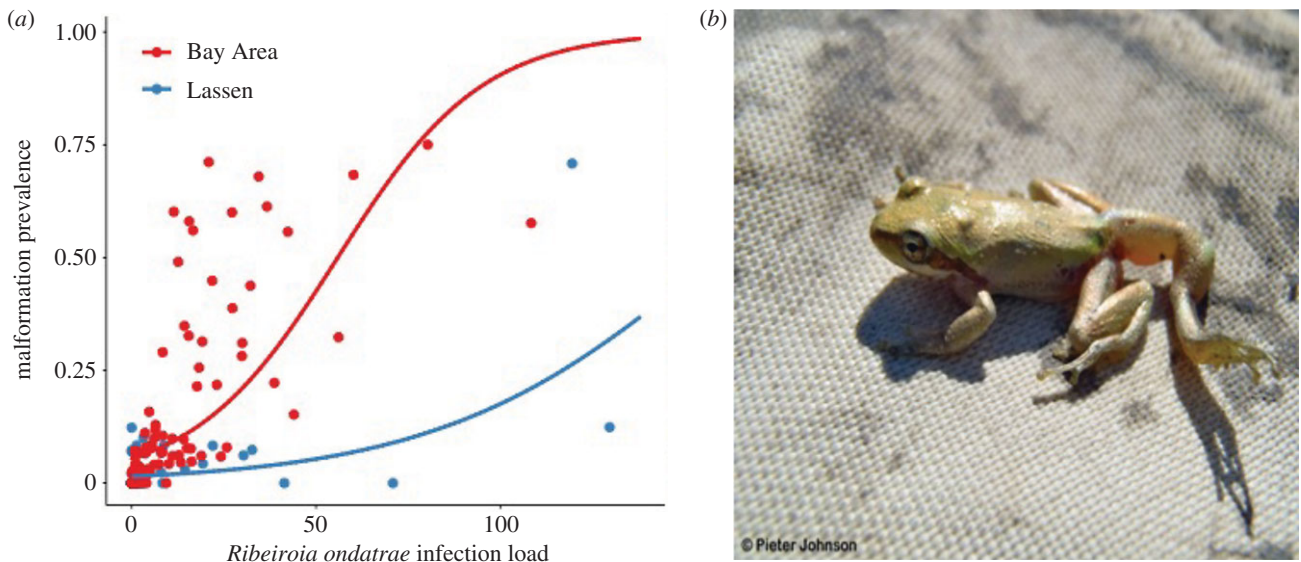


Figure 1. (a) Amphibian developmental malformations have been closely linked with infection levels of the trematode *R. ondatrae*, yet the specific relationship varies across location. For example, in Bay Area of California (red dots and line), infection of *R. ondatrae* is positively associated with malformations (scaled infection load 1.15 ± 0.05 , $p < 0.0001$), yet this relationship is largely diminished in habitats around Mt Lassen (blue dots and line) (scaled infection load: Lassen: -0.55 ± 0.06 , $p < 0.0001$). Each point represents a site by year observation of mean infection load and site level malformation prevalence which is defined as the proportion of recently metamorphic frogs that have a developmental malformation, such as is shown in (b). (Online version in colour.)

the timing in which this interaction occurs [18,19]. For example, fungal infections of bats exhibit a strong seasonal dependency, for which host mortality risk is greatest during hibernation periods that provide optimal temperatures for fungal growth [18]. Thus, it is critical to understand how sensitive host and parasite interactions are to any shifts in either of the host or parasite's phenology, as research has shown this can result in host switching [20], or alter co-infection patterns [21]; however, there has been limited work addressing how these phenological shifts alter host pathology. Because parasite-induced host pathology often dictates host fitness and influences transmission [22–24], phenologically driven changes in host pathology can result in cascading effects on the ecology and evolutionary trajectories of host and parasite taxa.

Parasites with free-living environmental stages may be especially likely to exhibit differential shifts in phenology relative to their hosts [16,19]. Particularly when outside of the host environment, free-living infectious stages can be highly sensitive to temperature changes, which often dictate development time or replication rate [25,26]. For instance, even relatively small changes in temperature can cause helminth parasites to develop faster, exhibit more generations per year, or be released earlier, which in some cases leads to more or earlier host infections [27–29]. However, determining how such changes impact the resulting pathology depends critically on the degree of synchrony between parasite infectious stages and the availability of susceptible hosts. Because both host susceptibility to infection and vulnerability to parasite-induced pathology vary with time (e.g. seasonality), mismatches in host–parasite phenology can alter pathology even if total parasite infection abundance remains constant [30–32]. For example, release of parasites earlier in the season could increase infection pressure during highly vulnerable host stages, thereby resulting in more pathology, host death or infection of novel host species [32]. Alternatively, if host phenological advancement outpaces that of their parasites, infections during less vulnerable or more resistant host life stages might reduce pathology [23].

In the western USA, widespread observations of frogs with severe limb deformities, including extra limbs, extra digits and skin webbings (figure 1), have been linked to infection by the digenetic flatworm, *Ribeiroia ondatrae* [33–36]. Malformations, which can affect as much as 90% of emerging frogs in some populations, are a potential conservation concern, given that affected individuals rarely survive to maturity [37,38]. Across both experimental studies and large-scale field surveys, higher *R. ondatrae* infection loads are functionally linked to a greater frequency of malformations among metamorphosing frogs [33–35]. Yet, there is also remarkable variation in this relationship across populations [38]. Among amphibian populations at higher elevation, including long-term study sites around Mt Lassen in California (e.g. [34]), the slope of the relationship between *R. ondatrae* infection and malformation frequency is 43% lower than for populations of the same amphibian host species at lower elevations, despite a similar range in infection (figure 1a). The most likely explanation for this disparity involves the phenological synchrony between host and parasite: for *R. ondatrae* to cause developmental malformations, its infectious stages (which are released by aquatic snails) must infect a larval amphibian within a 'critical window' of early limb development; earlier infections often result in host death, whereas later infections are unlikely to cause malformations [19]. Thus, in environments with a shorter growing season, even slight asynchronies between host and parasite could reduce the likelihood of infection during the critical window, leading to fewer or more variable patterns in pathology.

To investigate the influence of phenological synchrony between hosts and parasites in shaping patterns of host pathology (limb malformations), we intensively sampled populations of amphibian hosts and their trematode parasites between two regions that differ in elevation by approximately 1500 m (Bay Area and Mt Lassen). While both regions support the same host and parasite species, their contrast offers a natural phenological gradient owing to elevational and climatic differences [39,40] (figure 2a). From larval development

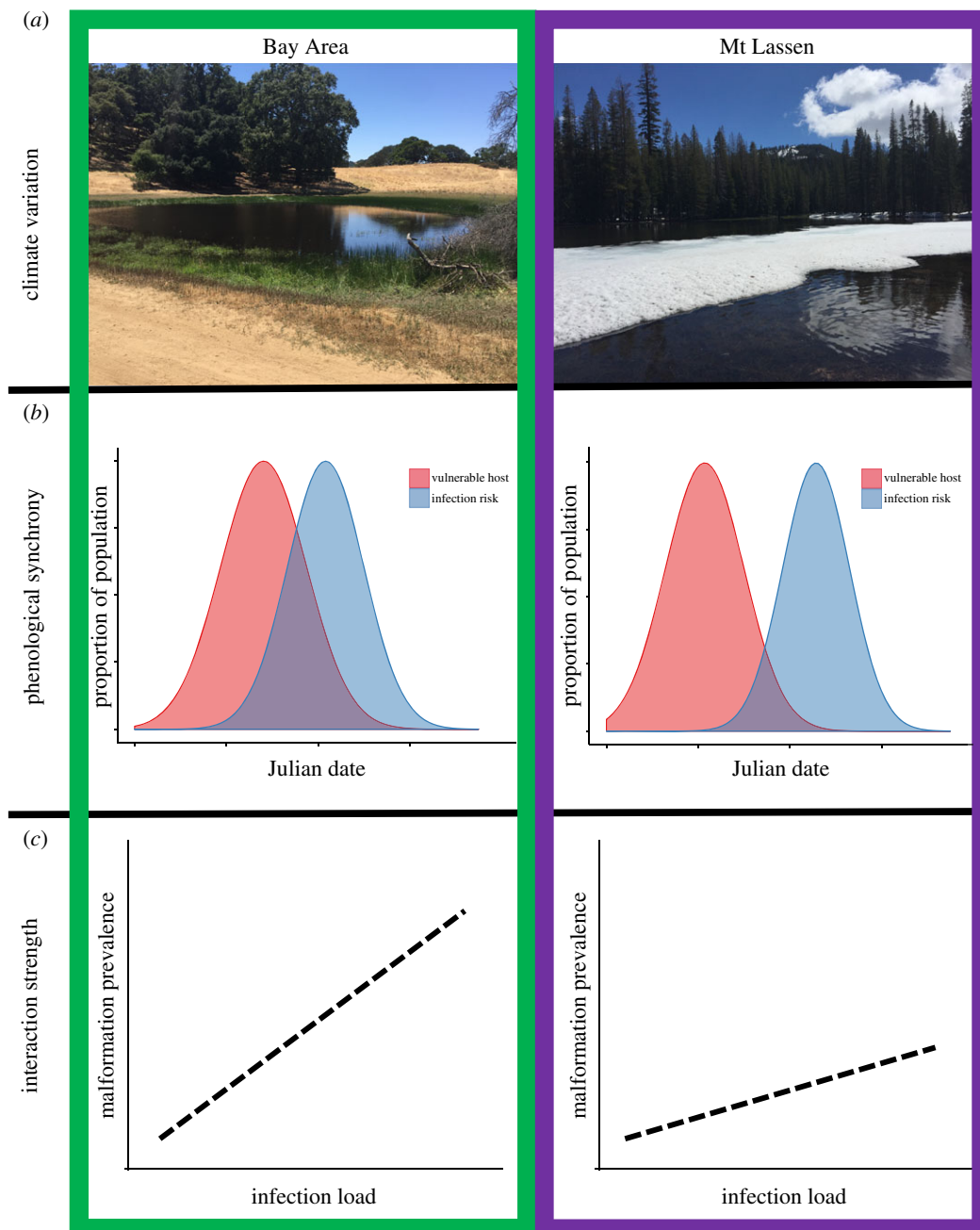


Figure 2. The two study locations in our system Bay Area (red box) and Mt Lassen area (blue box) vary substantially in their climate which can ultimately shape the phenological patterns of each system and resultant interaction strengths. (a) In the Bay Area, late winter/early spring rains promote amphibian egg laying, whereas in Mt Lassen area, ponds ice over in the winter and amphibian egg laying does not start till ponds are ice free starting in later spring/early summer. In both systems, the amphibians developing throughout the summer season and as the water warms, the developing amphibians experience an increase in infection risk as parasites begin to get released from their snail host. (b) However, the relative level of phenological synchrony between host and infection risk in these systems can vary due to differences in late winter and spring climate patterns. (c) This variation in phenological synchrony can impact the resultant interaction strength, where higher phenological synchrony results in higher pathology as host are getting infected during more vulnerable stages compared with systems with lower phenological synchrony. (Online version in colour.)

through metamorphosis, we assessed how differences in the phenology of host–parasite interactions dictated patterns in infection prevalence, parasite load and pathology. If variation in phenological synchrony drives malformations, we predicted that sites with a high proportion of synchrony between infection and the proportion of hosts in the critical window would support higher disease pathology, even after controlling for infection load (figure 2*b,c*). Our study thus aimed to evaluate how variation in parasite–host phenological synchrony alters not only disease dynamics but also the resultant host pathology.

2. Material and methods

(a) Field surveys

We sampled host populations within small ponds in California across the San Francisco Bay Area and the Mt Lassen portion of the Southern Cascades. Both locations have an established history of malformed amphibians linked to *R. ondatrae* infections [34,38]. *A priori*, we expected these locations to vary in the phenology of developing amphibians and parasites due to differences in elevation (maximum site-level elevations—Bay Area: 492 m, Mt Lassen: 2007 m above sea level) and weather in

early spring (mean high March temperature—Bay Area 15.5°C, Mt Lassen 10.5°C) (figure 2a). These temperature differences are associated with contrasts in the timing of egg laying by Pacific chorus frogs (*Pseudacris regilla*) [41,42], which is a lentic-breeding species that is a highly competent host for *R. ondatrae* (e.g. [34]). In the Bay Area, *P. regilla* breeding usually occurs from late January until early May, whereas in high elevation sites such as Mt Lassen, breeding occurs after ice clears from the ponds, typically from late May to early July [41]. For both locations, tadpoles develop over several months and metamorphose in the same year, often around mid-June to late August in the Bay and mid-August to early September in Lassen.

Ribeiroia ondatrae is a digenetic trematode that uses three hosts to complete its life cycle [43]. Parasite eggs deposited along with the faeces of its bird definitive host, typically wading birds or ducks, help disperse the parasite among ponds. The eggs hatch in water and infect its first intermediate host, a freshwater snail in the family Planorbidae, within which it undergoes asexual reproduction leading to the release of free-living infectious stages. These cercariae then infect a second intermediate host, typically developing amphibians or fish, which are then transmitted into the definitive host when a bird consumes an infected amphibian or fish. The production of cercariae is influenced by temperature [25], such that release often begins in late spring or early summer and continues until early autumn until temperature drops and the parasite overwinters inside the snail [43]. As a result, larval amphibians are exposed to infectious cercariae during their developmental season.

During the spring and summer of 2017, we surveyed ten ponds in the Bay Area and six in Mt Lassen across *P. regilla* developmental period (five to six visits per pond). Pond selection was determined based on previous surveys detecting both *P. regilla* malformations and *R. ondatrae* infections (P.T.J.J. 2016, unpublished data). In the Bay Area, sampling initiated in late March, whereas for Mt Lassen, the initial sampling event was in mid-June after ice thaw. To quantify variation in infection patterns, we randomly collected 15 developing *P. regilla* on each visit to determine *R. ondatrae* infection status and load through quantitative necropsy [35]. To determine variation in *P. regilla* development (i.e. what fraction were within the ‘critical window’ of vulnerability to malformations), we quantified the distribution of developmental stage of approximately 25 randomly sampled tadpoles [44]. Following Johnson *et al.* [19], a developing tadpole was considered within the ‘critical window’ if it was between stages 24 and 37. At the final visit, we recorded malformation prevalence by examining approximately 100 post-metamorphic *P. regilla* for limb anomalies (figure 1). Finally, to monitor differences in pond temperature between the study areas, we installed temperature loggers (HOBO Pendant Data Logger) 10 cm below the surface of each pond to record temperature hourly.

(b) Statistical analysis

(i) Phenological analysis

To assess how phenological patterns of vulnerable hosts varied across sites, we modelled changes in the proportion of developing *P. regilla* within the vulnerable ‘critical window’ across time and locations. To characterize how phenological patterns of infection risk varied between regions, we took a two-step approach: first, we modelled the proportion of hosts infected with *R. ondatrae* across time and locations. We then calculated infection risk by extracting the line of best fit for infection prevalence over time for each site and taking the derivative. Thus, the corresponding metric represents the rate of change in infection prevalence, for which high values correspond to a rapid increase in infection prevalence. This measure of parasite phenology helped capture variation in the timing of infection within amphibian hosts. The use of alternative metrics, such as the density of

R. ondatrae-infected snails, yielded less information about the timing of actual infections within hosts, given that transmission from snail to amphibian intermediate hosts is often nonlinear [45] and shaped by a range of habitat characteristics such as pond shape or predator abundances [46]. Similarly, metrics such as infection intensity per amphibian host would have limited our ability to disentangle the respective influences of, and interaction between, infection load and infection timing in driving host pathology (see below). The proportions of infected and vulnerable hosts were modelled as binomial responses using the `cbind` function in R to account for unequal sample size. Julian date of the visit and its interaction with location (Bay Area or Mt Lassen) were included as fixed-effect predictors.

We constructed generalized linear mixed models (GLMMs) using a binomial distribution with a logit link function and site identity as a random intercept term. Models were built using the package `lme4` [47] in the R programming language [48]. For both models, a significant interaction between date and location would indicate differential phenological patterns of parasite exposure or host development. To assess how temperature influenced these patterns, we reran the models with the date-specific mean water temperature for each site to evaluate whether temperature was a better predictor than date and location. To quantify how changes in the phenological pattern alter when in the development period the host get infected, we modelled how individual hosts varied in infection prevalence or load relative to amphibian developmental stage (e.g. Gosner stages). We used GLMMs with scaled Gosner stage of individual *P. regilla* and its interaction with location as predictors and random intercept terms for site identity and visit number (as a categorical variable). Prevalence was modelled using a binomial distribution for the error response while infection load was modelled using a Poisson distribution with an observation-level random effect to account for overdispersion.

(ii) Quantifying phenological synchrony

To quantify the degree of phenological synchrony between peak *R. ondatrae* infection risk and the proportion of developing *P. regilla* within the vulnerable ‘critical window’, we first extracted the predicted changes of both responses across the sampling period from the best-fit phenological models. Then we calculated the shared area (i.e. the degree of synchrony) under the two curves (see darker shaded area in figure 2b). To account for differences in the range of values, we scaled infection risk to the maximum change in infection prevalence across time for each location, where a value of 1 represents peak infection risk during the developmental season. Thus, both peak infection risk and the proportion of vulnerable hosts provided equal ranges for comparing the phenological phenomena. The degree of phenological synchrony therefore also ranged from 0 to 1, and characterized the proportion of observed infection occurring during the vulnerable stages. This term was used as a main effect and as an interaction term with parasite infection load in analyses of pathology (see below). Multiplying phenological synchrony by mean infection load functions to create a measure of ‘effective parasite load’, or those infections with the potential to induce pathology.

(iii) Parasite-induced pathology

Finally, we evaluated how phenological synchrony moderated the relationship between parasite infection load and the risk of developmental malformations in amphibians. While average parasite load is a well-established predictor of malformation risk, we tested how the measure of phenological synchrony derived above functioned to alter the strength of this link. In essence, low values of synchrony suggest a lower ‘effective parasite load’ and thus a reduced risk of pathology, given that infections occurred outside of the critical window. Statistically,

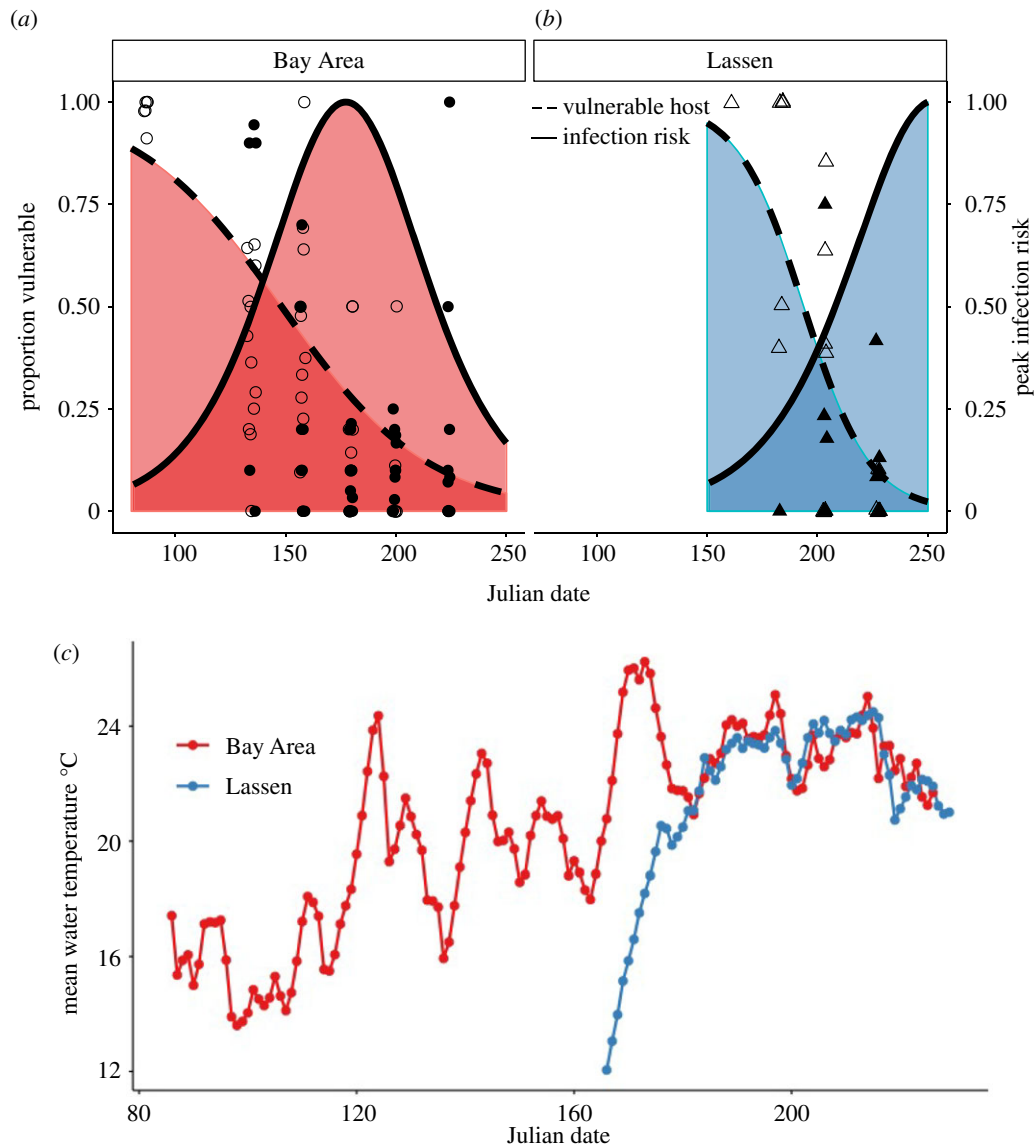


Figure 3. (a) Phenological patterns of vulnerable *P. regilla* within the ‘critical windows’ for malformations (dotted line) and infection risk of *R. ondatrae* (solid line) across the Bay Area (each red circles represent a unique site visit with open circles illustrating the proportion of the population within the vulnerable critical window and the solid circles the scaled proportional change in the population infected with *R. ondatrae* from previous sampling event) and the Lassen area (each blue triangle represents a unique site visit with open triangles illustrating the proportion of the population within the vulnerable critical window and the solid triangles the proportion of the population infected with *R. ondatrae*). In the Bay Area, the vulnerable *P. regilla* decreased gradually across the summer season as the infection prevalence steadily rose. This resulted in a mean phenological synchrony (darker shaded overlapped area) of 0.53 ± 0.09 . This was higher than the synchrony in Lassen (b), where we observed a faster decrease in the vulnerable *P. regilla* (scaled Julian date: Lassen: -1.80 ± 0.61 , $p = 0.003$) and similar patterns of increase in infection patterns resulting in a mean phenological synchrony of 0.41 ± 0.08 . (c) The differences in the decrease in vulnerable *P. regilla* could not be explained by difference in temperature (mean water temperature: -0.07 ± 0.17 , $p = 0.68$), as once the Lassen area sites warmed up, they quickly reach similar levels as sites within the Bay Area. (Online version in colour.)

we evaluated how the mean *R. ondatrae* infection load per host interacted with phenological synchrony to determine malformation prevalence, modelled using a binomial distribution and the logit link function with a generalized linear model (GLM). We also included region (Bay Area or Mt Lassen) as a main effect. After building the initial model, we removed non-significant predictors sequentially based if they had a significance greater than 0.05 in likelihood-ratio tests.

3. Results

(a) Phenology analysis

Developing *P. regilla* amphibians exhibited sharply different phenological patterns between Mt Lassen and the Bay Area. While the proportion of vulnerable hosts declined steadily across the summer period for both locations (GLMM: scaled

Julian date: -0.99 ± 0.11 , $p = 0.0001$) (figure 3), host availability in Mt Lassen sites declined at a faster rate (scaled Julian date: Lassen -1.80 ± 0.61 , $p = 0.03$). These patterns were not due to differences in the mean water temperature (mean water temperature: -0.07 ± 0.17 , $p = 0.68$). We did not observe significant differences in the phenology of *R. ondatrae* infection prevalence between regions as both locations exhibited similar rates of increasing infection prevalence (scaled Julian date: 2.08 ± 0.10 , $p = 0.001$) (figure 3). However, we did observe differences in the overall infection prevalence with lower values in Lassen compared with the Bay Area (Lassen: -3.10 ± 1.32 , $p < 0.001$).

By extracting the slope for vulnerable host availability and the calculated infection risk over time, we determined the degree of phenological synchrony for each site and in both regions (electronic supplementary material, S1). Overall,

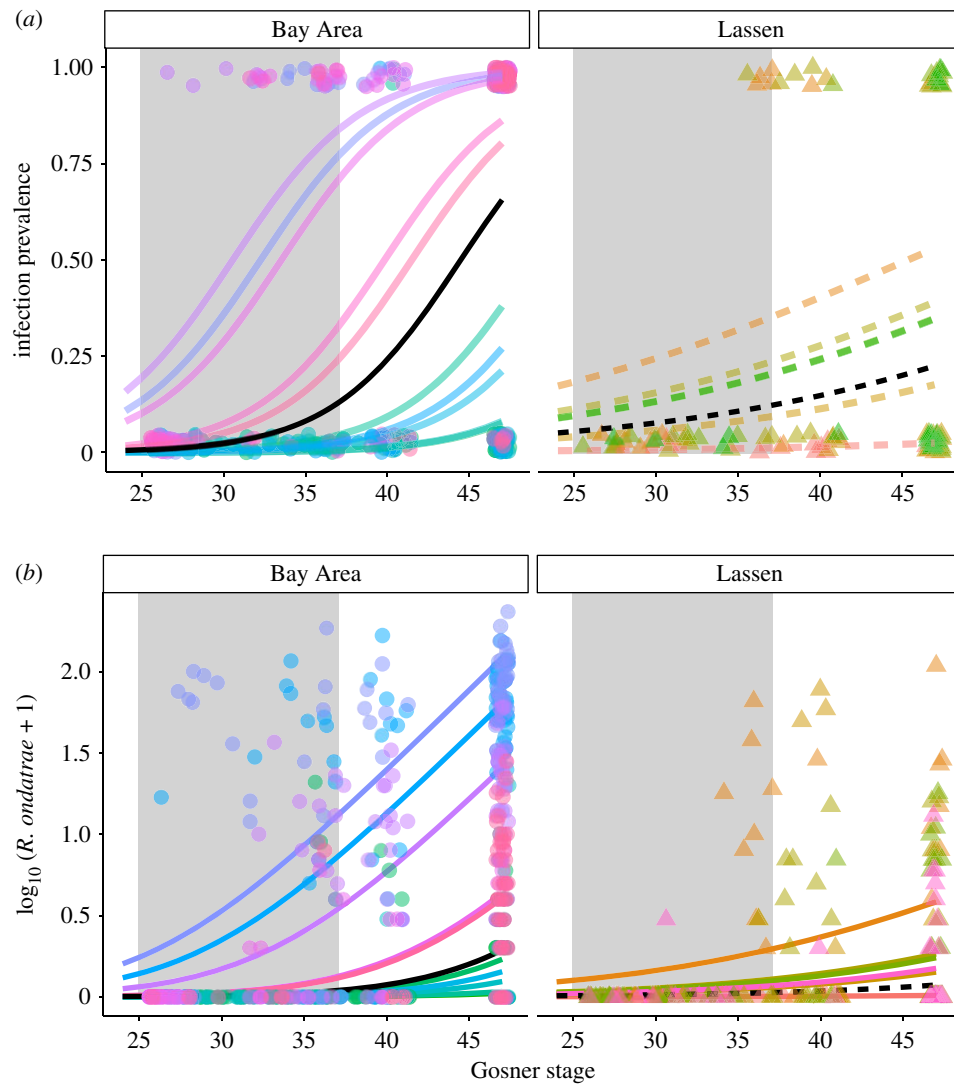


Figure 4. Patterns of infection prevalence and load across different developmental stages between the Bay Area (left) and Lassen (right). Each coloured line represents a unique site and the solid black lines represent the mean trend for the two areas. Each coloured data point represents an individual frog from the corresponding sites colour. The faded grey boxes represent the 'critical window' of development where the *P. regilla* are vulnerable to malformations. (a) Developing *P. regilla* in the Bay Area were more likely to be infected by *R. ondatrae* at earlier stages than *P. regilla* in the Lassen area (Gosner stage: Lassen -1.38 ± 0.27 , $p < 0.00001$). (b) We see similar patterns in infection load with higher infection load within the 'critical window' of vulnerability in the Bay Area relative to Lassen (Gosner stage: Lassen -0.92 ± 0.26 , $p < 0.001$). (Online version in colour.)

the Bay Area had higher phenological synchrony, with a mean value (± 1 s.e.) of 0.53 ± 0.09 , compared to Mt Lassen with a mean of 0.41 ± 0.08 . In the Bay Area, site-level synchrony ranged from 0.21 to 0.87 relative to 0.15 to 0.63 for Mt Lassen. Correspondingly, we observed broad differences in the relationship between infection (probability and load) and host developmental stages between the two regions. In the Bay Area, *P. regilla* had a higher probability of infection (infection probability GLMM—Mt Lassen: Gosner stage: -1.37 ± 0.27 , $p < 0.00001$) and higher infection loads (infection load GLMM—Lassen: Gosner stage: -0.93 ± 0.26 , $p = 0.0004$) at earlier host developmental stages compared to similarly staged host individuals found in Mt Lassen (figure 4). As a result, developing hosts at the last stage of the 'critical window' (Gosner stage 37) had an average infection load of 8.48 ± 1.29 in the Bay Area compared to 2.22 ± 0.29 in Mt Lassen.

(b) Pathology patterns

Across all sites, the frequency of amphibian limb malformations ranged from 0 to 75%, with the highest level

observed at a Bay Area pond ($n = 100$ individuals examined). Overall, malformation frequency increased with the mean infection load (malformation GLM—scaled \log_{10} transformed infection load: 0.91 ± 0.33 , $p = 0.005$), as expected. However, the rate of increase was strongly mediated by the degree of phenological synchrony (malformation GLM—scaled \log_{10} transformed infection load: scaled phenological synchrony: 1.50 ± 0.24 , $p < 0.00001$) (figure 5). Thus, a 30% change in the degree of host/parasite phenological synchrony can lead to 100-fold increase in malformation prevalence when the mean infection is about 50 metacercariae per frog. The best-fitting model included the mean infection load, phenological synchrony, and their interaction (for full model results, see electronic supplementary material, S2), with no additional effect of location after accounting for these terms.

4. Discussion

Climate-induced shifts in phenological synchrony between species can shape the outcome of species interactions

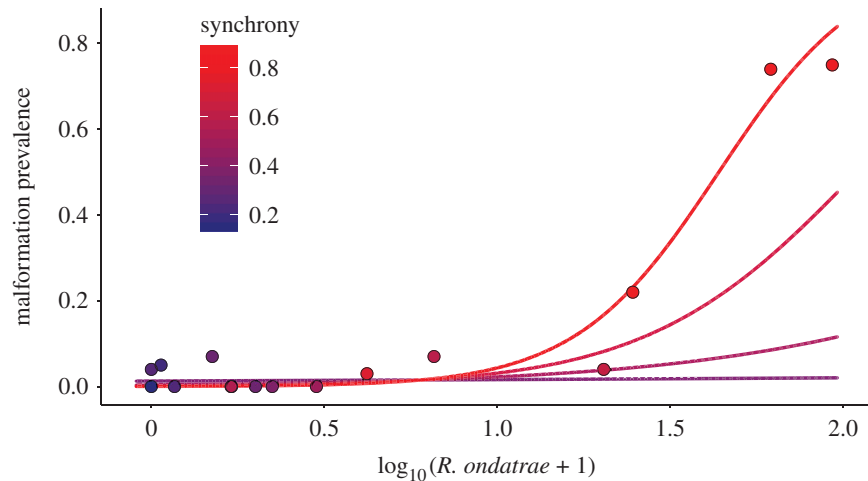


Figure 5. Overall malformation prevalence correlated positively with site-level infection load (scale *R. ondatrae* infection load: 0.91 ± 0.33 , $p = 0.005$), yet the specific relationship was mediated by the degree of phenological synchrony (scale *R. ondatrae* infection load: synchrony: 1.50 ± 0.24 , $p < 0.0001$). Each dot represents a unique site of the study with its corresponding mean infection level (x-axis) as well its malformation prevalence (y-axis). The colour represents the degree of phenological synchrony with warmer colours representing higher synchrony. Each line represents the predicted relationship between infection load and malformation levels under different phenological synchrony values ranging from 0.31 to 0.63. Our result shows that to obtain high levels of malformations, there needs to be a synergistic effect high infection loads and high levels of phenological synchrony. (Online version in colour.)

[7,10,12], including those between hosts and parasites. In this study, we illustrate how the degree of phenological synchrony between vulnerable hosts and parasite risk alters parasite load, infection prevalence and ultimately host pathology. Building upon earlier experimental work (see [19]), our analytical models and field-based comparisons between locations differing in climate and phenology highlight the joint importance of parasite exposure as well as the timing of host–parasite interactions in controlling host pathology in natural populations, offering insights into how a changing climate may shift the strength and outcome of host–parasite interactions.

A major challenge in assessing the consequences of phenological shifts on species interactions is identifying the taxon-specific responses of potentially interacting organisms. In situations where interacting species experience asynchronous phenological shifts, even minor perturbations in climate or circadian cues can result in considerable alterations in interaction strength [3,9]. Based on the current study of amphibian–trematode interactions between regions that contrasted in elevation, we observed sharply differing phenological overlap between vulnerable amphibian hosts and infectious parasites. More specifically, the timing of infection risk by the trematode *R. ondatrae* was similar across both study areas, with low infection risk early in the amphibian developmental season that increased through the summer months as warming waters enhanced the release of free-living infectious stages from snail hosts and peaking in the Bay Area around late June/early July and mid-August in Lassen [25]. Although water temperatures in the Bay Area were warmer early in the season, once Mt Lassen ponds became ice-free the temperature rapidly increased to become comparable (figure 3c). The core difference between the two regions involved the development of amphibian larvae, and in particular, the availability of hosts within the vulnerable window corresponding to early limb development [45]. Thus, in the Bay Area, the proportion of vulnerable *P. regilla* larvae declined slowly across the summer, whereas in Mt Lassen, the vulnerable host declined more than twice

as fast, regardless of study site (figure 3). This differential pattern in amphibian phenology could be driven by either differences in the development rate of larval hosts or variation in the number of deposited cohorts within the community. We found little evidence for variation in development rates, given that water temperatures, which are one of the main drivers of tadpole growth and development, were consistent between location [49]. More likely, the core difference between regions involved the number of overlapping cohorts, which directly influenced the availability of tadpole hosts within the vulnerable developmental window; in the Bay Area, for instance, *P. regilla* begins breeding during the rainy season and may range from February through at least early May [42]. This results in numerous, staggered developmental cohorts, maintaining higher variation in developmental stage (figure 4). At higher elevations, by contrast, *P. regilla* often breed in a single event after waterbodies become ice free [41], leading to less heterogeneity in developmental stage range and a more synchronous decline in the proportion of vulnerable hosts. The net effect is a smaller temporal window for *R. ondatrae* to infect and ultimately cause host pathology, likely result in boom and bust years for the frequency of malformations.

Across both locations, ponds with higher levels of phenological synchrony had higher levels of infections during vulnerable stages of host development (figure 4), resulting in an increased likelihood of developmental malformations (figure 5) [19]. As *P. regilla* in the Bay Area, on average, supported higher levels of phenological synchrony, they correspondingly exhibited a greater per-parasite risk of malformation. Indeed, on average, each established parasite in the Bay Area had a 33% higher probability of causing limb malformations compared to infections in the Mt Lassen area. For hosts in Mt Lassen, a greater fraction of their sustained infection loads were acquired after they emerged beyond the critical window of susceptibility, such that the slope of the relationship between infection intensity and malformation frequency was considerably weaker. Nonetheless, these results suggest that amphibian populations in

Mt Lassen likely experience substantial among-year variation in disease risk: because *P. regilla* in Lassen typically breed in a single burst [42], any increases in phenological synchrony should result in increased malformation prevalence. Years in which Lassen experience high levels of malformations were likely those in which synchrony between vulnerable host and infection by *R. ondatrae* were high. Because malformed amphibians rarely survive to adulthood [33], such events could affect long-term population dynamics and viability. As a result, it is important to identify and quantify how specific climatic factors shape synchrony to forecast how climate changes may alter host pathology and ultimately impact host populations.

Our study further illustrates how variation in phenological synchrony between interacting species can be driven by the shape of temporal overlap of both taxa, rather than just the changes in a single metric such as egg-laying date. For example, taxa that exhibit staggered breeding behaviour should have a broader distribution of developmental stages across time, resulting in a larger temporal window in which vulnerable hosts are available. By contrast, taxa that have a single breeding event will experience a more uniform distribution of their developmental stages through time, yielding a relatively short period during which vulnerable hosts are available. Thus, even small shifts in the phenology could drive a profound alteration in the corresponding interaction strengths. As a consequence, systems with highly synchronized phenological patterns should be more sensitive to shifting phenologies relative to communities that tend to promote lower synchronization [50,51].

A key priority for the future is to understand how climate-based factors shape host and parasite phenology with the aim of forecasting changes in synchrony across a range of host–parasite systems. Yet for many systems, we know relatively little about disease phenology, limiting opportunities to characterize how the timing of infection alters pathology patterns. While addressing these gaps will require intensive field sampling approaches, adopting analytical approaches that facilitate inferences about parasite–host

interaction strength in relation to climatic variables may help identify target systems in which to concentrate additional study. As phenological shifts are likely to continue in a warming world, it will further be important to consider how these changes alter local, regional and global distributions of parasites and pathogens, including the potential for novel host shifts and range expansions. Additionally, both hosts and parasites may adapt to these new phenological patterns, with potential implications for host evolution of resistance and tolerance to parasites. Identifying areas that may become more susceptible to infection or disease will facilitate management of outbreaks, and we highlight the value of research quantifying how the phenological synchrony of different parasite and host interactions respond to forecasted changes in climate.

Ethics. The data collection from animals was approved by the Institutional Animal Care and Use Committee at the University of Colorado.

Data accessibility. Data available from the Dryad Digital Repository: <https://doi.org/10.5061/dryad.wpzgmsbh8> [52].

Authors' contributions. T.M.-G., W.E.M., D.M.C. and P.T.J.J. designed the study. T.M.-G., W.E.M. and D.M.C. collected the data. T.M.-G. and P.T.J.J. analysed the data and T.M.-G. wrote the initial draft and all authors edited and provided feedback on the manuscript.

Competing interests. We declare we have no competing interests.

Funding. This work was supported by the United States Department of Agriculture Forest Services (grant no. 17-CS-11050600-015), the National Science Foundation (grant nos DEB 1149308 and 1754171), the National Institutes of Health (grant no. R10 GM109499) and the David and Lucile Packard Foundation.

Acknowledgements. We acknowledge Tom Rickman and his staff of the Forest Service for his logistical and sampling assistance in collecting data from the Lassen area. We thank East Bay Regional Parks for access to sites. We also thank D. Mckittrick and S. Goodnight for their assistance in the field and thank T. Riepe, K. Leslie and A. Shah for their assistance in dissection. We thank the members of the Johnson laboratory, especially K. Loria, B. Hobart and T. Stewart-Merrill for their feedback on early drafts of the manuscript. We also thank two anonymous reviewers who greatly improved this manuscript with their comments and suggestions.

References

- Walther GR, Post E, Convey P, Menzel A, Parmesan C, Beebee TJ, Fromentin JM, Hoegh-Guldberg O, Bairlein F. 2002 Ecological responses to recent climate change. *Nature* **416**, 389–395. (doi:10.1038/416389a)
- Visser ME, Both C. 2005 Shifts in phenology due to global climate change: the need for a yardstick. *Phil. Trans. R. Soc. B* **272**, 2561–2569. (doi:10.1098/rspb.2005.3356)
- Kharouba HM, Ehrlén J, Gelman A, Bolmgren K, Allen JM, Travers SE, Wolkovich EM. 2018 Global shifts in the phenological synchrony of species interactions over recent decades. *Proc. Natl Acad. Sci. USA* **115**, 5211–5216. (doi:10.1073/pnas.1714511115)
- Parmesan C. 2007 Influences of species, latitudes and methodologies on estimates of phenological response to global warming. *Global Change Biol.* **13**, 1860–1872. (doi:10.1111/j.1365-2486.2007.01404.x)
- CaraDonna PJ, Iler AM, Inouye DW. 2014 Shifts in flowering phenology reshape a subalpine plant community. *Proc. Natl Acad. Sci. USA* **111**, 4916–4921. (doi:10.1073/pnas.1323073111)
- Pureswaran DS, De Grandpré L, Paré D, Taylor A, Barrette M, Morin H, Regniere J, Kneeshaw DD. 2015 Climate-induced changes in host tree–insect phenology may drive ecological state-shift in boreal forests. *Ecology* **96**, 1480–1491. (doi:10.1890/13-2366.1)
- Carter SK, Saenz D, Rudolf VH. 2018 Shifts in phenological distributions reshape interaction potential in natural communities. *Ecol. Lett.* **21**, 1143–1151. (doi:10.1111/ele.13081)
- Gordo O. 2007 Why are bird migration dates shifting? A review of weather and climate effects on avian migratory phenology. *Clim. Res.* **35**, 37–58. (doi:10.3354/cr00713)
- Thackeray SJ *et al.* 2016 Phenological sensitivity to climate across taxa and trophic levels. *Nature* **535**, 241–245. (doi:10.1038/nature18608)
- Yang LH, Rudolf VHW. 2010 Phenology, ontogeny and the effects of climate change on the timing of species interactions. *Ecol. Lett.* **13**, 1–10. (doi:10.1111/j.1461-0248.2009.01402.x)
- Alexander JM, Levine JM. 2019 Earlier phenology of a nonnative plant increases impacts on native competitors. *Proc. Natl Acad. Sci. USA* **116**, 199–204. (doi:10.1073/pnas.1820569116)
- Deacy WW, Armstrong JB, Leacock WB, Robbins CT, Gustine DD, Ward EJ, Erlenbach JA, Stanford JA. 2017 Phenological synchronization disrupts trophic interactions between Kodiak brown bears and salmon. *Proc. Natl Acad. Sci. USA* **114**, 10 432–10 437. (doi:10.1073/pnas.1705248114)
- Patz JA, Campbell-Lendrum D, Holloway T, Foley JA. 2005 Impact of regional climate change on human

- health. *Nature* **438**, 310–317. (doi:10.1038/nature04188)
14. Harvell CD, Mitchell CE, Ward JR, Altizer S, Dobson AP, Ostfeld RS, Samuel MD. 2002 Climate warming and disease risks for terrestrial and marine biota. *Science* **296**, 2158–2162. (doi:10.1126/science.1063699)
15. Anderson PK, Cunningham AA, Patel NG, Morales FJ, Epstein PR, Daszak P. 2004 Emerging infectious diseases of plants: pathogen pollution, climate change and agrotechnology drivers. *Trends Ecol. Evol.* **19**, 535–544. (doi:10.1016/j.tree.2004.07.021)
16. Altizer S, Dobson A, Hosseini P, Hudson P, Pascual M, Rohani P. 2006 Seasonality and the dynamics of infectious diseases. *Ecol. Lett.* **9**, 467–484. (doi:10.1111/j.1461-0248.2005.00879.x)
17. Brooks DR, Hoberg EP. 2007 How will global climate change affect parasite–host assemblages? *Trends Parasitol.* **23**, 571–574. (doi:10.1016/j.pt.2007.08.016)
18. Langwig KE *et al.* 2015 Host and pathogen ecology drive the seasonal dynamics of a fungal disease, white-nose syndrome. *Phil. Trans. R. Soc. B* **282**, 20142335.
19. Johnson PTJ, Kellermanns E, Bowerman J. 2011 Critical windows of disease risk: amphibian pathology driven by developmental changes in host resistance and tolerance. *Funct. Ecol.* **25**, 726–734. (doi:10.1111/j.1365-2435.2010.01830.x)
20. Hoberg EP, Brooks DR. 2008 A macroevolutionary mosaic: episodic host-switching, geographical colonization and diversification in complex host–parasite systems. *J. Biogeogr.* **35**, 1533–1550. (doi:10.1111/j.1365-2699.2008.01951.x)
21. Halliday FW, Umbanhowar J, Mitchell CE. 2017 Interactions among symbionts operate across scales to influence parasite epidemics. *Ecol. Lett.* **20**, 1285–1294. (doi:10.1111/ele.12825)
22. De Roode JC, Yates AJ, Altizer S. 2008 Virulence–transmission trade-offs and population divergence in virulence in a naturally occurring butterfly parasite. *Proc. Natl Acad. Sci. USA* **105**, 7489–7494. (doi:10.1073/pnas.0710909105)
23. Kuris AM. 2003. Evolutionary ecology of trophically transmitted parasites. *J. Parasitol.* **89**, 96–100.
24. Svensson EI, Råberg L. 2010 Resistance and tolerance in animal enemy–victim coevolution. *Trends Ecol. Evol.* **25**, 267–274. (doi:10.1016/j.tree.2009.12.005)
25. Paull SH, LaFonte BE, Johnson PTJ. 2012 Temperature-driven shifts in a host–parasite interaction drive nonlinear changes in disease risk. *Global Change Biol.* **18**, 3558–3567. (doi:10.1111/gcb.12018)
26. Molnár PK, Dobson AP, Kutz SJ. 2013 Gimme shelter—the relative sensitivity of parasitic nematodes with direct and indirect life cycles to climate change. *Global Change Biol.* **19**, 3291–3305. (doi:10.1111/gcb.12303)
27. Hudson PJ, Cattadori IM, Boag B, Dobson AP. 2006. Climate disruption and parasite–host dynamics: patterns and processes associated with warming and the frequency of extreme climatic events. *J. Helminthol.* **80**, 175–182. (doi:10.1079/JOH2006357)
28. Paull SH, Johnson PTJ. 2014 Experimental warming drives a seasonal shift in the timing of host–parasite dynamics with consequences for disease risk. *Ecol. Lett.* **17**, 445–453. (doi:10.1111/ele.12244)
29. Gethings OJ, Rose H, Mitchell S, Van Dijk J, Morgan ER. 2015 Asynchrony in host and parasite phenology may decrease disease risk in livestock under climate warming: *Nematodirus battus* in lambs as a case study. *Parasitology* **142**, 1306–1317. (doi:10.1017/S0031182015000633)
30. Poulin R. 2011 *Evolutionary ecology of parasites*. Princeton, NJ: Princeton University Press.
31. Kelly DW, Thomas H, Thielges DW, Poulin R, Tompkins DM. 2010 Trematode infection causes malformations and population effects in a declining New Zealand fish. *J. Anim. Ecol.* **79**, 445–452. (doi:10.1111/j.1365-2656.2009.01636.x)
32. Gehman AM, Hall RJ, Byers JE. 2018 Host and parasite thermal ecology jointly determine the effect of climate warming on epidemic dynamics. *Proc. Natl Acad. Sci. USA* **115**, 744–749. (doi:10.1073/pnas.1705067115)
33. Johnson PTJ, Lunde KB, Ritchie EG, Launer AE. 1999 The effect of trematode infection on amphibian limb development and survivorship. *Science* **284**, 802–804. (doi:10.1126/science.284.5415.802)
34. Johnson PTJ *et al.* 2002 Parasite (*Ribeiroia ondatrae*) infection linked to amphibian malformations in the western United States. *Ecol. Monogr.* **72**, 151–168. (doi:10.1890/0012-9615(2002)072[0151:PROILT]2.0.CO;2)
35. Johnson PTJ, Preston DL, Hoverman JT, Richgels KL. 2013 Biodiversity decreases disease through predictable changes in host community competence. *Nature* **494**, 230–234. (doi:10.1038/nature11883)
36. Lunde KB, Johnson PTJ. 2012 A practical guide for the study of malformed amphibians and their causes. *J. Herpetol.* **46**, 429–442. (doi:10.1670/10-319)
37. Goodman BA, Johnson PTJ. 2011 Disease and the extended phenotype: parasites control host performance and survival through induced changes in body plan. *PLoS ONE* **6**, e20193. (doi:10.1371/journal.pone.0020193)
38. Lunde KB, Resh VH, Johnson PTJ. 2012 Using an ecosystem-level manipulation to understand host–parasite interactions and how they vary with study venue. *Ecosphere* **3**, 1–18. (doi:10.1890/ES12-00001.1)
39. Hopkins AD. 1920 The bioclimatic law. *J. Wash. Acad. Sci.* **10**, 34–40.
40. Vandvik V, Halbritter AH, Telford RJ. 2018 Greening up the mountain. *Proc. Natl Acad. Sci. USA* **115**, 833–835. (doi:10.1073/pnas.1721285115)
41. Schaub DL, Larsen Jr JH. 1978 The reproductive ecology of the Pacific treefrog (*Hyla regilla*). *Herpetologica* **34**, 409–416.
42. Stebbins RC. 2003 *A field guide to western reptiles and amphibians*. New York, NY: Houghton Mifflin Harcourt.
43. Johnson PTJ, Sutherland DR, Kinsella JM. 2004 Pathogenesis with special emphasis on the amphibian malformation problem. *Adv. Parasitol.*, **57**, 181–2523.
44. Gosner KL. 1960 A simplified table for staging anuran embryos and larvae with notes on identification. *Herpetologica* **16**, 183–190.
45. Orlofsky SA, Flaxman SM, Joseph MB, Fenton A, Melbourne BA, Johnson PTJ. 2018 Experimental investigation of alternative transmission functions: quantitative evidence for the importance of nonlinear transmission dynamics in host–parasite systems. *J. Anim. Ecol.* **87**, 703–715. (doi:10.1111/1365-2656.12783)
46. Rohr JR *et al.* 2015 Predator diversity, intraguild predation, and indirect effects drive parasite transmission. *Proc. Natl Acad. Sci. USA* **112**, 3008–3013. (doi:10.1073/pnas.1415971112)
47. Bates D, Maechler M, Bolker B, Walker S. 2013 *lme4: Linear mixed-effects models using Eigen and S4*. R package version, 1.0–5.
48. R Development Team. 2013 *R: a language and environment for statistical computing*. Version 3.1.3. Vienna, Austria: R Foundation for Statistical Computing.
49. Harkey GA, Semlitsch RD. 1988 Effects of temperature on growth, development, and color polymorphism in the ornate chorus frog *Pseudacris ornata*. *Copeia* **1988**, 1001–1007. (doi:10.2307/1445724)
50. Defriez EJ, Reuman DC. 2017 A global geography of synchrony for terrestrial vegetation. *Glob. Ecol. Biogeogr.* **26**, 878–888. (doi:10.1111/geb.12595)
51. Carter SK, Rudolf VH. 2019 Shifts in phenological mean and synchrony interact to shape competitive outcomes. *Ecology* **100**, e02826. (doi:10.1002/ecy.2826)
52. McDevitt-Galles T, Moss WE, Calhoun DM, Johnson PTJ. 2020 Data from: Phenological synchrony shapes pathology in host–parasite systems. Dryad Digital Repository. (doi:10.5061/dryad.wpzgmsb8h)